Hybrid DWNN-RF Framework for EEG-Based Autism Spectrum Disorder Detection: A Low-Complexity and Interpretable Approach

Flávio Secco Fonseca
Dept. Engenharia da Computação
Universidade de Pernambuco
Recife, Brazil
fsf2@ecomp.poli.br

Jordana Leandro Seixas
Dept. Engenharia da Computação
Universidade de Pernambuco
Recife, Brazil
jls3@ecomp.poli.br

Adrielly Sayonara de Oliveira Silva
Dept. de Engenharia Biomédica
Universidade Federal de Pernambuco
Recife, Brazil
adrielly.sayonara@ufpe.br

Fábio Matheus Spindola da Cunha
Dept. de Engenharia Biomédica
Universidade Federal de Pernambuco
Recife, Brazil
fabio.matheus@ufpe.br

Maiara Marçal Araújo
Dept. de Engenharia Biomédica
Universidade Federal de Pernambuco
Recife, Brazil
maiara.maraujo@ufpe.br

Ana Carolina Soares de Melo
Dept. de Engenharia Biomédica
Universidade Federal de Pernambuco
Recife, Brazil
carolina.soaresm@ufpe.br

Maíra Araújo de Santana
Dept. de Engenharia Biomédica
Universidade Federal de Pernambuco
Recife, Brazil
mas2@ecomp.poli.br

Cecilia Cordeiro da Silva
Dept. de Engenharia Biomédica
Universidade Federal de Pernambuco
Recife, Brazil
cecilia.csilva@ufpe.br

Clarisse Lins de Lima
Dept. de Engenharia Biomédica
Universidade Federal de Pernambuco
Recife, Brazil
clarisse.lins@ufpe.br

Arianne Sarmento Torcate
Dept. Engenharia da Computação
Universidade de Pernambuco
Recife, Brazil
ast@ecomp.poli.br

Giselle Machado Magalhães Moreno
Dept. de Engenharia Biomédica
Universidade Federal de Pernambuco
Recife, Brazil
giselle.moreno@ufpe.br

Juliana Carneiro Gomes
Dept. de Engenharia Biomédica
Universidade Federal de Pernambuco
Recife, Brazil
juliana.cgomes@ufpe.br

Wellington Pinheiro dos Santos
Dept. de Engenharia Biomédica
Universidade Federal de Pernambuco
Recife, Brazil
wellington.santos@ufpe.br

***Abstract*—Autism Spectrum Disorder (ASD) is a complex neurodevelopmental condition characterized by challenges in social interaction, communication, and repetitive behaviors. The diagnostic process for ASD remains challenging due to the heterogeneity of symptoms and reliance on subjective clinical evaluations, often leading to delayed interventions. Early and precise diagnosis is critical for enabling timely therapeutic support and improving developmental outcomes. In this study, we propose a novel hybrid methodology for ASD detection using electroencephalographic (EEG) signals. Our approach integrates Deep-Wavelet Neural Networks (DWNN) for feature extraction with Random Forest classifiers for robust decision-making. DWNNs leverage predefined wavelet filter banks, eliminating the need for parameter tuning and reducing computational complexity while capturing both temporal and spectral patterns in EEG data. This architecture not only ensures efficient feature extraction but also operates sustainably without requiring GPU acceleration, making it suitable for resource-constrained environments. Experimental results demonstrate the effectiveness of our hybrid model, achieving an accuracy of 82.0%, a kappa index of 0.640, sensitivity of 96.0%, and specificity of 68.0% when using a Random Forest with 500 trees. These findings highlight the potential of DWNN-based frameworks in providing accurate, reliable, and interpretable solutions for ASD diagnosis, paving the way for scalable and sustainable AI-driven healthcare applications.**

***Index Terms*—Autism Spectrum Disorder (ASD), Electroencephalography (EEG), Deep-Wavelet Neural Network, Random Forest Classifier, Health Informatics, Neuroengineering**

I. Introduction

Autism Spectrum Disorder (ASD) consists of a neurodevelopmental conditions characterized by challenges in social interaction, communication, and the presence of repetitive behaviors or restricted interests [1]. The diagnostic process for ASD is considerably complex due to the heterogeneity of symptoms and the reliance on subjective clinical evaluations,

which can lead to variability in diagnosis and delayed interventions [2]. Early and precise diagnosis is crucial for providing timely therapeutic interventions that can significantly enhance the developmental trajectories of individuals with ASD [1], [2].

In recent years, advancements in technology have played an increasingly vital role in advancing diagnostic procedures for neurodevelopmental disorders. Among the various tools available, electroencephalography (EEG) has emerged as a valuable non-invasive method for neurological assessment [3]–[5]. EEG's ability to capture the electrical activity of the brain offers a window into the neural correlates of ASD, potentially allowing for more objective diagnostic indicators [3], [6]. Nevertheless, the complexity of EEG signals necessitates sophisticated analytical techniques to discern meaningful patterns associated with ASD.

Deep learning, particularly through transfer learning, provides a robust framework for this task. Transfer learning allows the leveraging of pre-trained models, which have been developed on extensive datasets, to adapt and excel in new, related domains with fewer training samples [7]–[9]. This approach is particularly advantageous in the context of ASD diagnosis, where the richness of EEG data requires a nuanced and powerful feature extraction mechanism.

In recent years, EEG analysis has benefited from the development of more efficient feature extraction techniques. Among them, Deep-Wavelet Neural Networks (DWNNs) stand out for combining the mathematical rigor of wavelet theory with the hierarchical representation capabilities of deep learning. By employing predefined wavelet filters, DWNNs eliminate the need for parameter tuning, enabling low-complexity, interpretable, and efficient feature extraction—especially suitable for biomedical signals such as EEG.

In this paper, we present a novel methodology for Autism Spectrum Disorder (ASD) detection using electroencephalographic (EEG) signals. Our approach employs a hybrid deep learning architecture that leverages Deep-Wavelet Neural Networks (DWNN) for feature extraction and Random Forests for classification. DWNNs are innovative deep learning architectures inspired by wavelet decomposition and Mallat's algorithm, which eliminate the need for training or parameter adjustment since they utilize predefined wavelet coefficients as fixed filter banks. This characteristic not only reduces computational complexity but also ensures robustness in extracting hierarchical features from EEG signals, capturing both temporal and spectral patterns associated with ASD. By integrating DWNN with Random Forests, our hybrid model achieves a balance between sophisticated feature representation and interpretable classification, offering a promising solution for automated ASD diagnosis.

II. Related Works

A. EEG-Based Techniques for ASD Diagnosis

Electroencephalography (EEG) has been increasingly utilized in the pursuit of objective markers for Autism Spectrum Disorder (ASD) diagnosis. Peketi and Dhok [10] tackled the challenge of detecting the P300 signal in EEG recordings from individuals with ASD, employing Variational Mode Decomposition (VMD) to handle the non-stationary nature of the signals. This approach demonstrated an accuracy of 91.12%, marking a significant step forward in EEG analysis for ASD. Similarly, Kang et al. [11] combined EEG with eye-tracking data, achieving an accuracy of up to 85.44%. Their work revealed the potential of multimodal data fusion in capturing the multifaceted nature of ASD. More recently, Abdulhay et al. [12] explored the EEG ripple range (75–250 Hz), achieving an accuracy of 98.9% and shedding light on the effectiveness of this underexplored frequency range for ASD diagnosis.

B. Deep Learning in Health Informatics

Deep learning has revolutionized health informatics, providing powerful tools for analyzing complex medical datasets. In the context of ASD, Mohi ud Din and Jayanthy [13] utilized Second-Order Wavelet Transform coefficients as inputs to Long Short Term Memory (LSTM) and Convolutional Neural Networks (CNN), achieving diagnostic accuracies of 94% and 92%, respectively. This study exemplifies the potential of deep learning to interpret intricate patterns in EEG signals. Meanwhile, Al-Qazzaz et al. [14] proposed a hybrid model that combined a pre-trained CNN with a Support Vector Machine (SVM), resulting in 87.8% accuracy. Their work underscores the growing trend of using deep learning hybrids to enhance diagnostic precision in the realm of biomedical engineering.

C. Deep-Wavelet Neural Networks

Deep-Wavelet Neural Networks (DWNN) represent a novel approach to feature extraction in image analysis, particularly in the domain of biomedical imaging. Unlike traditional deep learning models that rely heavily on gradient-based optimization and extensive computational resources, DWNNs leverage predefined wavelet filter banks, eliminating the need for parameter adjustment during training [15], [16]. This unique characteristic not only reduces computational complexity but also makes DWNNs highly efficient and accessible, even in environments without access to high-performance computing or GPU acceleration [15], [16].

DWNNs are inspired by wavelet decomposition and Mallat's algorithm, which decompose images into multi-resolution components using fixed low-pass and high-pass filters. This process allows DWNNs to capture both spatial and frequency-domain information effectively, making them particularly suited for tasks requiring detailed pattern recognition, such as lesion detection and classification in medical images [15], [16]. Each layer of the DWNN applies the predefined filter bank to the input image, followed by downsampling to reduce resolution and data complexity [15], [16]. This iterative process continues through multiple layers, with each layer providing deeper levels of feature extraction.

A key distinction of DWNNs is their independence from gradient descent-based training methods [15], [16]. While traditional deep learning architectures, such as Convolutional Neural Networks (CNNs), require significant computa-

tional resources for backpropagation and weight adjustments, DWNNs operate with fixed orthogonal filters derived from wavelet theory [15], [16]. This eliminates the dependency on GPU acceleration and reduces energy consumption, making DWNNs an attractive alternative for applications where computational efficiency and sustainability are critical [15]–[17].

DWNNs have demonstrated consistent performance in breast cancer diagnosis using mammographic and thermographic images. For instance, Barbosa et al. [15] investigated the use of DWNNs for feature extraction from thermographic images, achieving accuracies exceeding 98% in detecting and classifying breast lesions [15]. Their work highlighted the ability of DWNNs to analyze images in both spatial and frequency domains, capturing intricate patterns associated with malignancies. Similarly, Santana and dos Santos [16] applied a six-layer DWNN to extract attributes from regions of interest in mammograms, achieving an average accuracy of 94% and a kappa index of 0.91 when combined with a second-degree polynomial kernel support vector machine (SVM) [16]. These results underscore the effectiveness of DWNNs in transforming complex image data into a feature space where simpler classifiers can achieve high performance.

One of the most significant advantages of DWNNs over traditional CNNs is their reliance on predefined wavelet filter banks, which eliminates the need for extensive training and parameter tuning [15]–[17]. This makes DWNNs particularly advantageous in scenarios with limited labeled data, such as biomedical applications. Additionally, DWNNs mitigate the risk of overfitting and memory overload by reducing the dimensionality of feature maps through downsampling operations at each layer. Comparative studies have shown that DWNNs outperform state-of-the-art CNN architectures like Inception V3, MobileNet, ResNet50, VGG16, VGG19, and Xception in terms of accuracy, sensitivity, specificity, and precision, all while operating with significantly lower computational demands.

The absence of gradient-based optimization in DWNNs also translates to reduced energy consumption, addressing a growing concern in the deployment of deep learning systems. Traditional deep learning models often require powerful GPUs and high-performance computing clusters, which consume substantial amounts of energy [15]–[17]. In contrast, DWNNs can be implemented on standard CPUs, making them a sustainable and cost-effective solution for resource-constrained settings, such as rural healthcare facilities or developing countries [15]–[17]. By bridging the gap between advanced signal processing techniques and deep learning, DWNNs pave the way for scalable, sustainable, and accessible AI-driven healthcare solutions.

III. Materials and Methods

The methodological approach applied in this work will be presented below, with each step illustrated in the diagram of Fig. 1. We will start by detailing the dataset, followed by the preprocessing steps, then the training, validation, and testing of the algorithms, and finally the analysis of the results.

A. Data Collection

This study used EEG data obtained from the Sheffield database [18], which included information from 56 participants evenly split between individuals diagnosed with Autism Spectrum Disorder (ASD) and neurotypical participants, ranging in age from 18 to 68 years. The EEG signals were recorded using the Biosemi Active Two system over 150 seconds, during which participants rested with their eyes closed and were exposed to visual stimuli. Electrode configurations ranged from 64 to 128 channels; however, for consistency in analysis, all recordings were standardized to 64 channels, with Cz as the reference electrode. A band-pass filter from 0.01 to 140 Hz was also applied to improve data quality.

B. Preprocessing of EEG Signals

The EEG signals went through a series of preprocessing steps to ensure they were clean and ready for analysis. Initially, unwanted artifacts and noise were filtered out using EEGLAB [19], with a band-pass filter set to include a 1 Hz transition band. Any data segments showing significant distortions were removed, and the entire dataset was resampled at 512 Hz for consistency.

To extract features, the signals were divided into 5-second windows, overlapping by 1 second. Each segment's signals from different channels were combined and transformed into image representations using the Fast Wavelet Transform (FWT). This was done with Mallat's algorithm and Daubechies 8 (db8) filter banks [20], chosen for their ability to highlight important multi-resolution patterns in the EEG data, which could be useful for identifying ASD-related features.

C. Feature extraction

After windowing, we converted the signals into spectrogram images represented in the time-frequency domain using the Wavelet Transform. This approach enables the capture of dynamic frequency variations within the signal, which is particularly useful for EEG analysis, as brain activity involves oscillations that change rapidly over time.

Next, from each spectrogram, we extracted features using a Deep Wavelet Neural Network (DWNN) configured with four layers and synthesis blocks for minimum, maximum, mean, and median operations. This hybrid architecture leverages the wavelet transform's ability to decompose complex signals into different frequency levels, while deep neural networks learn relevant patterns and features for classification.

This combination aimed to extract meaningful characteristics from EEG images while optimizing the classification process to better capture the specific EEG patterns associated with ASD. We investigated the following classifiers: Bayes Net, Naive Bayes, Random Tree, J48 decision tree, and Random Forest with 100, 200, 300, 400, and 500 trees.

D. Experimental Setup

The data was split into two groups: one for training and validation, making up 80% of the total (401 samples), and another for testing, which accounted for the remaining 20%

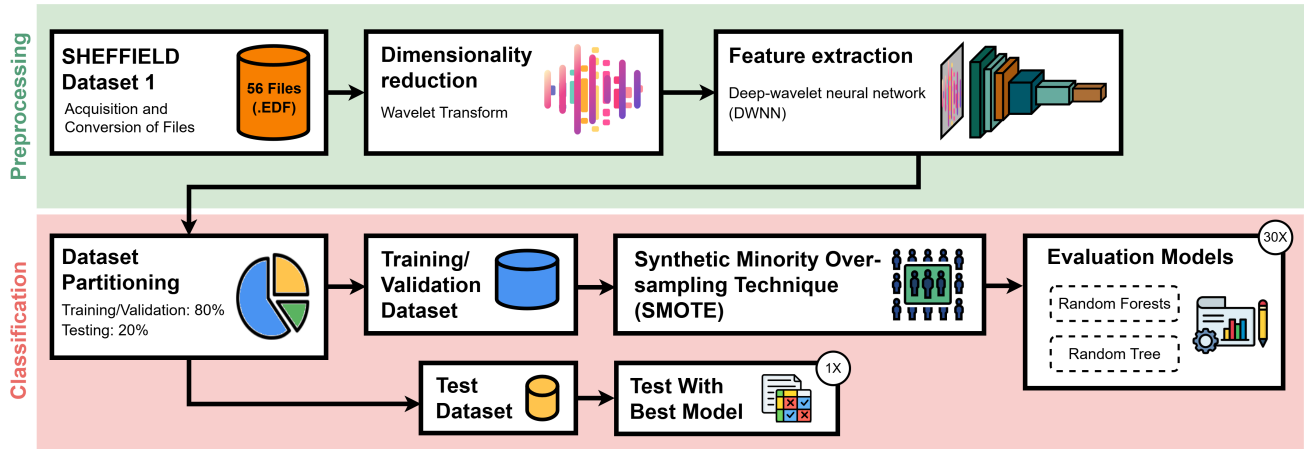

Fig. 1. Diagram illustrating the applied methodological flow: 1) Dataset; 2) Dimensionality reduction using wavelet transform; 3) Feature extraction with DWNN; 4) Division of the base into training, validation and testing; 5) Oversampling of the training base; 6) Algorithm training; 7) Testing of the best model.

(100 samples). To improve training and reduce variability, the training-validation set was expanded by generating synthetic samples using the Synthetic Minority Over-sampling Technique (SMOTE) method [21]. After augmentation, the training set increased to 1203 instances, maintaining a balanced class distribution (approximately 50%-50%). This ensured that both ASD and control classes were equally represented during training, helping to prevent classifier bias towards the majority class and enhancing generalization.

The training and validation process was carried out using the augmented dataset, allowing for the evaluation of different classifier configurations. To ensure more robust results, the models underwent 10-fold cross-validation, repeated 30 times. Finally, the best model found was tested in a single round with its test base. The implementation and testing of the classifiers were performed using Weka software, version 3.8 [22].

The performance metrics used to evaluate the classifiers included accuracy, kappa statistic, sensitivity, specificity, and the area under the ROC curve (AUC-ROC). These metrics were selected because they provide a comprehensive assessment of classifier performance, capturing both precision and recall aspects of the predictions. Statistical analysis was performed to compare the performance of different classifier configurations.

E. Performance Metrics

To assess the effectiveness of the classifiers in the context of ASD diagnosis, we utilized a set of well-established performance metrics commonly used in machine learning and biomedical diagnostics. These metrics provide a comprehensive evaluation of classifier performance by considering different aspects of prediction outcomes. The mathematical definitions of these metrics are presented below, assuming a binary classification problem where TP represents True Positives, TN represents True Negatives, FP represents False Positives, and FN represents False Negatives.

Accuracy is a metric that measures the overall correctness of the classifier's predictions. It is defined as:

$$\text{Accuracy} = \frac{TP + TN}{TP + TN + FP + FN}. \tag{1}$$

The Kappa statistic measures inter-rater agreement or the agreement between the classifier's predictions and the actual results, taking into account the possibility that the agreement occurred by chance. It is defined as:

$$\kappa = \frac{p_o - p_e}{1 - p_e}. \tag{2}$$

where p_o is the observed agreement and p_e is the expected agreement by chance.

Sensitivity, also known as True Positive Rate or recall, measures the ability of the classifier to correctly identify positive cases. It is defined as:

$$\text{Sensitivity} = \frac{TP}{TP + FN}. \tag{3}$$

Specificity measures the ability of the classifier to correctly identify negative cases. It is defined as:

$$\text{Specificity} = \frac{TN}{TN + FP}. \tag{4}$$

The Area Under the ROC Curve (AUC-ROC) is a performance measure that considers the classifier's ability to distinguish between classes at various threshold settings. The ROC curve plots the True Positive Rate (TPR) against the False Positive Rate (FPR), and the AUC represents the degree of separability.

$$\text{AUC-ROC} = \int_0^1 \text{TPR}(FPR^{-1}(t))\, dt. \tag{5}$$

To ensure a stable and reliable assessment of classifier performance, these metrics were computed for each fold during the cross-validation process and then averaged over 30 runs. The selection of these metrics was driven by the need to evaluate both overall accuracy and the classifiers' ability to correctly diagnose ASD, especially given the potential class imbalance in the dataset.

IV. Results

The performance of different classifiers was assessed using the metrics outlined in Section III-E. A summary of the results is provided in Table I, which displays the mean and standard deviation for accuracy, kappa statistic, sensitivity, specificity and AUC-ROC across all tested classifier configurations. Additionally, Fig. 2 and 3 illustrate the variation of the kappa index and AUC-ROC in relation to different classifier settings.

TABLE I
CLASSIFICATION PERFORMANCE OF THE EVALUATED ALGORITHMS DURING TRAINING AND VALIDATION. THE TABLE PRESENTS MEAN VALUES AND STANDARD DEVIATIONS FOR ACCURACY, SENSITIVITY, SPECIFICITY, KAPPA INDEX, AND AUC ACROSS MULTIPLE CROSS-VALIDATION RUNS, HIGHLIGHTING THE COMPARATIVE PERFORMANCE AND STABILITY OF EACH MODEL CONFIGURATION.

	Classifier	Accuracy (%)	Kappa	Sensitivity	Specificit	AUC
Mean	Bayes Net	63.4	0.270	0.964	0.306	0.639
	Naive Bayes	15.6	0.366	0.254	0.984	0.552
	J48	84.3	0.687	0.851	0.835	0.859
	Random Tree	78.3	0.566	0.784	0.782	0.783
	RF-100	95.9	0.919	0.998	0.921	0.997
	RF-200	96.6	0.933	0.999	0.934	0.998
	RF-300	96.8	0.936	0.999	0.937	0.999
	RF-400	97.0	0.939	0.999	0.940	0.999
	RF-500	97.0	0.940	0.999	0.940	0.999
Standard deviation	Bayes Net	3.19	0.0636	0.0255	0.0586	0.0312
	Naive Bayes	2.97	0.438	0.371	0.0276	0.0616
	J48	3.49	0.0699	0.0494	0.0501	0.0375
	Random Tree	4.05	0.0811	0.0536	0.0576	0.0405
	RF-100	1.95	0.0390	0.00611	0.0387	0.00339
	RF-200	1.70	0.0341	0.00456	0.0338	0.00262
	RF-300	1.64	0.0328	0.00340	0.0328	0.00256
	RF-400	1.61	0.0323	0.00340	0.0322	0.00262
	RF-500	1.58	0.0316	0.00314	0.0318	0.00274

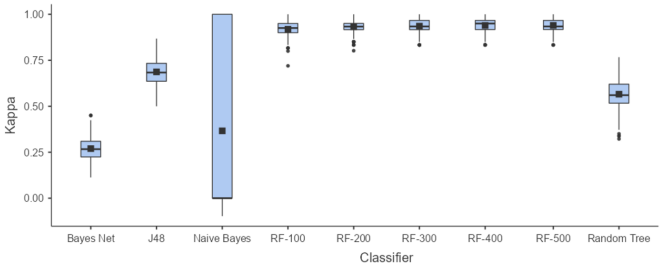

Fig. 2. Kappa index according to classifiers' configurations, where RF n represents a Random Forest with n trees.

The Random Forest with 400 and 500 trees (RF-400 and RF-500) achieved the highest accuracy (97.0%) and the highest AUC-ROC values (0.999), indicating excellent predictive capability and model robustness. Additionally, they had the lowest standard deviations, which suggests stability in predictions across multiple runs. The J48 (decision tree) achieved 84.3% accuracy but had a higher standard deviation (3.49%), indicating greater variability in the results. Naive Bayes showed a much lower performance (15.6%) with a standard deviation of 2.97%, revealing that, in addition to low performance, the model exhibits significant fluctuation in results. Bayes Net (63.4%) had a moderate performance but was not very reliable, as its standard deviation (3.19%) indicates instability. Random Tree, although a simplified version of Random Forest, with 78.3% accuracy and a standard deviation of 4.05%, had the highest variation among the tested methods, suggesting that its predictions are more affected by small changes in the data.

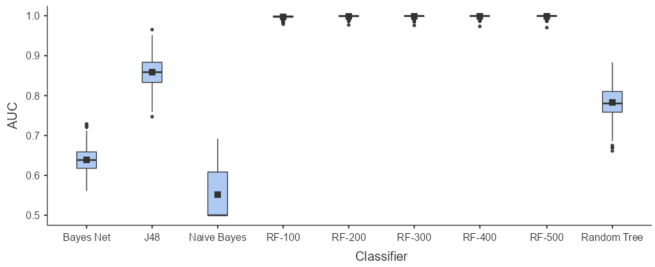

Fig. 3. Area under ROC curve (AUC-ROC) according to classifiers' configurations, where RF n represents a Random Forest with n trees.

The Random Forest models (RF-100 to RF-500) exhibited very high sensitivity (0.999) with extremely low standard deviations (0.00314 to 0.00611). This means that the model can correctly identify almost all positive ASD cases while maintaining high stability across executions. The specificity of the RF models ranged from 0.921 to 0.940, with reduced standard deviations (0.0318 to 0.0387), indicating a good balance between identifying positive and negative cases.

The kappa index measures the agreement between predictions and actual labels, accounting for chance. In this metric, the Random Forest models (RF-100 to RF-500) achieved the best results, with values above 0.919 and low variation (standard deviation up to 0.0316), ensuring consistent predictions. The J48 model (kappa = 0.687, standard deviation = 0.0699) showed intermediate performance, while Naive Bayes (kappa = 0.366, standard deviation = 0.438) exhibited significant fluctuation, making it unreliable. The Random Tree model (kappa = 0.566, standard deviation = 0.0811) also demonstrated instability. Thus, RF-400 and RF-500 stand out as the most robust and reliable options.

The AUC-ROC evaluates a model's ability to distinguish between classes. In this analysis, the Random Forest models (RF-100 to RF-500) achieved near-perfect scores, ranging from 0.997 to 0.999, with low standard deviations between 0.00256 and 0.00339, confirming their strong performance and consistency. The J48 model, with an AUC-ROC of 0.859 and a standard deviation of 0.0375, showed reasonable effectiveness but with greater variability. Naive Bayes, on the other hand, performed poorly, with an AUC-ROC of 0.552 and a higher standard deviation of 0.0616, indicating weak separation between classes. The Random Tree model showed intermediate results, with an AUC-ROC of 0.783 and a standard deviation of 0.0405. Given these findings, the Random Forest models continue to be the most effective and reliable choice for this classification task.

Table II presents the results obtained by the RF-500 model

during the testing phase, using an independent dataset not seen during training or validation. This final evaluation aimed to assess the generalization capability of the model in a realistic diagnostic scenario, simulating how it would perform when applied to new EEG data from unseen individuals.

TABLE II
PERFORMANCE METRICS OF THE RANDOM FOREST MODEL WITH 500 TREES (RF-500) IN THE TESTING PHASE. THE TABLE SUMMARIZES THE MODEL'S ABILITY TO GENERALIZE TO UNSEEN DATA, INCLUDING ACCURACY, SENSITIVITY, SPECIFICITY, COHEN'S KAPPA COEFFICIENT, AND THE AREA UNDER THE ROC CURVE (AUC).

	Accuracy (%)	Sensitivity	Specificity	Kappa	AUC
RF-500	82.0	0.96	0.68	0.64	0.90

The confusion matrix, in Fig. 4, shows that the model correctly classified 48 out of 50 individuals with ASD (true positives) and 34 out of 50 control individuals (true negatives). However, it misclassified 16 control cases as ASD (false positives) and failed to detect 2 ASD cases (false negatives). These results indicate that while the model is highly effective at identifying ASD cases, it struggles with some false-positive classifications. The accuracy of the model reached 82%, showing that the majority of classifications were correct. The sensitivity was 96%, confirming the model's strong ability to detect ASD cases. The specificity was lower at 68%, meaning that the model had more difficulty distinguishing control individuals, leading to a higher number of false positives.

The area under the ROC curve (AUC-ROC) of 0.90 confirms the model's strong ability to differentiate ASD and control cases, given its high sensitivity. The kappa index of 0.64 suggests substantial agreement beyond chance, reinforcing the model's reliability. However, the higher number of false positives suggests room for improvement, particularly in increasing specificity.

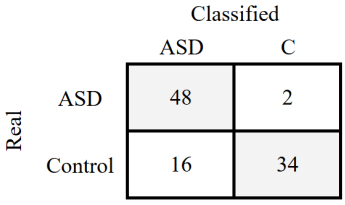

Fig. 4. Confusion matrix of the testing stage performed with the best model, Random Forest with 500 trees

V. DISCUSSION

The results obtained in this study highlight the importance of combining efficient feature extraction with interpretable classification models for EEG-based ASD diagnosis. Among all evaluated algorithms, Random Forest models, particularly those with 400 and 500 trees, consistently demonstrated superior performance in accuracy, kappa index, sensitivity, specificity, and AUC-ROC, with minimal variability across runs. These outcomes underscore the robustness and generalization capacity of ensemble-based classifiers when trained on wavelet-transformed EEG representations.

The excellent sensitivity observed (up to 99.9%) indicates the model's strong capacity to detect ASD-related patterns in EEG signals. However, the moderate specificity (approximately 68% in the testing phase) suggests a tendency to overclassify ASD cases, resulting in false positives. While this trade-off is common in health-related screening tasks—where higher sensitivity is often prioritized—it highlights a potential limitation for real-world deployment, especially in clinical contexts where specificity is critical to avoid unnecessary interventions.

Although Random Forests with 400 and 500 trees yielded the highest accuracy and stability, it is important to highlight that models with fewer trees, such as RF-100 and RF-200, also achieved competitive results, with differences of less than 1.5% in most metrics. Considering that Random Forest complexity increases with the number of trees—resulting in higher memory consumption and longer inference times—smaller models may be preferable in real-world applications, particularly in embedded or mobile systems. Therefore, the performance gains from RF-500 should be weighed against deployment constraints.

The use of Deep-Wavelet Neural Networks (DWNN) for feature extraction played a central role in the model's effectiveness. By eliminating the need for parameter tuning and leveraging fixed wavelet filter banks, DWNNs reduced computational cost while preserving critical time-frequency features. This design is particularly advantageous for deployment in resource-constrained environments, such as remote clinics or portable diagnostic systems.

Compared to recent studies in the literature, such as Abdulhay et al. [12] and Al-Qazzaz et al. [14], which report accuracies of 98.9% and 87.8%, respectively, the DWNN-RF hybrid architecture presents lower overall performance (82%). However, these approaches differ significantly in several aspects, including dataset composition, EEG acquisition protocols, and model complexity. For example, Abdulhay et al. [15] employed high-density EEG (64 channels), extensive preprocessing, and a custom neural network trained on the ripple frequency band—an approach that, while effective, depends on resources not commonly available in clinical settings. In contrast, our model emphasizes interpretability, low computational cost, and the use of standard EEG recordings, making it more suitable for deployment in low-resource environments. This trade-off between performance and practicality should be considered when comparing across studies.

Nonetheless, it is important to acknowledge that the use of a single dataset (Sheffield) limits the generalizability of the findings. Incorporating cross-dataset validation and diverse EEG acquisition protocols in future work would help reinforce the clinical applicability and robustness of the proposed framework.

VI. Conclusion

This study proposed a hybrid methodology for Autism Spectrum Disorder (ASD) detection using EEG signals, integrating Deep-Wavelet Neural Networks (DWNN) for feature extraction and Random Forest classifiers for decision-making. The DWNN approach enabled efficient, parameter-free extraction of time-frequency features, while Random Forest models provided robust classification with high interpretability.

Experimental results demonstrated that the Random Forest model with 500 trees achieved the best performance, with 82.0% accuracy, 96.0% sensitivity, 68.0% specificity, and a kappa index of 0.64 on the test set. These findings validate the effectiveness of the proposed framework in distinguishing ASD patterns in EEG data, especially in computationally constrained scenarios.

Future work will focus on increasing dataset diversity, evaluating generalization to multi-site EEG data, and exploring ensemble methods and adaptive wavelet strategies. The promising results reinforce the potential of combining wavelet-based signal analysis with interpretable machine learning models for scalable, non-invasive ASD diagnostic support.

Ultimately, this work contributes to the ongoing effort to develop objective, accessible, and computationally efficient tools for supporting early ASD diagnosis. By bridging wavelet-based signal analysis with interpretable machine learning, the proposed framework offers a scalable and sustainable solution with practical relevance for clinical environments—particularly those with limited computational resources. These findings encourage further exploration toward real-world deployment and integration into digital health systems.

Acknowledgment

This study was partially financed by the Financiadora de Estudos e Projetos - Brazil (FINEP, grant 2170.22). We are also grateful to Coordenação de Aperfeiçoamento de Pessoal de Nível Superior – Brazil (CAPES), Fundação de Amparo a Ciência e Tecnologia do Estado de Pernambuco - Brazil (FACEPE), and the National Council for Scientific and Technological Development - Brazil (CNPq), for the partial financial support.

References

[1] WHO, "Autism," 2023, accessed december, 2024. https://www.who.int/news-room/fact-sheets/detail/autism-spectrum-disorders.

[2] Y. Hus and O. Segal, "Challenges surrounding the diagnosis of autism in children," *Neuropsychiatric disease and treatment*, pp. 3509–3529, 2021.

[3] A. Chaddad, Y. Wu, R. Kateb, and A. Bouridane, "Electroencephalography signal processing: A comprehensive review and analysis of methods and techniques," *Sensors*, vol. 23, no. 14, p. 6434, 2023.

[4] M. K. Andrade, M. A. Santana, G. Moreno, I. Oliveira, J. Santos, M. C. A. Rodrigues, and W. P. dos Santos, *An EEG Brain-Computer Interface to Classify Motor Imagery Signals*. Singapore: Springer, 2020, pp. 83–98.

[5] A. P. S. de Oliveira, M. A. Santana, M. K. S. Andrade, J. C. Gomes, M. C. Rodrigues, and W. P. dos Santos, "Early diagnosis of parkinson's disease using eeg, machine learning and partial directed coherence," *Research on Biomedical Engineering*, vol. 36, no. 3, pp. 311–331, 2020.

[6] S. Bouazizi and H. Ltifi, "Enhancing accuracy and interpretability in eeg-based medical decision making using an explainable ensemble learning framework application for stroke prediction," *Decision Support Systems*, vol. 178, p. 114126, 2024.

[7] M. A. Santana, "Arquiteturas de redes profundas para interfaces musicais humano-máquina para reconhecimento de emoções em sinais eletroencefalográficos e de voz como apoio à musicoterapia," PhD thesis, Universidade de Pernambuco, Brazil, 2023. [Online]. Available: 10.13140/RG.2.2.22104.30725

[8] M. A. Santana and W. P. Santos, "Personalização de terapias pelo reconhecimento de emoções em biossinais," *Journal of Health Informatics*, vol. 16, no. Especial, 2024.

[9] M. A. Santana, F. S. Fonseca, A. S. Torcate, and W. P. dos Santos, "Emotion recognition from multimodal data: a machine learning approach combining classical and hybrid deep architectures," *Research on Biomedical Engineering*, vol. 39, no. 3, pp. 613–638, 2023.

[10] S. Peketi and S. B. Dhok, "Machine learning enabled p300 classifier for autism spectrum disorder using adaptive signal decomposition," *Brain Sciences*, vol. 13, no. 2, p. 315, 2023.

[11] J. Kang, X. Han, J. Song, Z. Niu, and X. Li, "The identification of children with autism spectrum disorder by svm approach on eeg and eye-tracking data," *Computers in biology and medicine*, vol. 120, p. 103722, 2020.

[12] E. Abdulhay, M. Alafeef, H. Hadoush, and N. Arunkumar, "A 64-channel scheme for autism detection via scaled conjugate gradient-based neural network classification of e lectroencephalogram ripples' complexity," *Expert Systems*, vol. 40, no. 4, p. e13000, 2023.

[13] Q. M. ud Din and A. K. Jayanthy, "Wavelet scattering transform and deep learning networks based autism spectrum disorder identification using eeg signals," *Traitement du Signal*, vol. 39, no. 6, p. 2069, 2022.

[14] N. K. Al-Qazzaz, A. A. Aldoori, A. Buniya, S. H. B. M. Ali, and S. A. Ahmad, "Transfer learning and hybrid deep convolutional neural networks models for autism spectrum disorder classification from eeg signals," *IEEE Access*, 2024.

[15] V. A. d. F. Barbosa, M. A. de Santana, M. K. S. Andrade, R. d. C. F. de Lima, and W. P. dos Santos, "Deep-wavelet neural networks for breast cancer early diagnosis using mammary termographies," in *Deep learning for data analytics*. Elsevier, 2020, pp. 99–124.

[16] M. A. de Santana and W. P. dos Santos, "A deep-wavelet neural network to detect and classify lesions in mammographic images," *Research on Biomedical Engineering*, vol. 38, no. 4, pp. 1051–1066, 2022.

[17] M. M. dos Santos, A. G. da Silva Filho, and W. P. dos Santos, "Deep convolutional extreme learning machines: Filters combination and error model validation," *Neurocomputing*, vol. 329, pp. 359–369, 2019.

[18] A. Dickinson, S. Jeste, and E. Milne, "Electrophysiological signatures of brain aging in autism spectrum disorder," *Cortex*, vol. 148, pp. 139–151, 2022.

[19] A. Delorme and S. Makeig, "Eeglab: an open source toolbox for analysis of single-trial eeg dynamics including independent component analysis," *Journal of neuroscience methods*, vol. 134, no. 1, pp. 9–21, 2004.

[20] S. G. Mallat *et al.*, "Multifrequency channel decompositions of images and wavelet models." *IEEE Trans. Acoustics, Speech, and Signal Processing*, vol. 37, no. 12, pp. 2091–2110, 1989.

[21] N. V. Chawla, K. W. Bowyer, L. O. Hall, and W. P. Kegelmeyer, "Smote: synthetic minority over-sampling technique," *Journal of artificial intelligence research*, vol. 16, pp. 321–357, 2002.

[22] I. H. Witten and E. Frank, *Data Mining: Pratical Machine Learning Tools and Technique*. San Francisco, CA, USA: Morgan Kaufmann Publishers, 2005.